Graphene-Based Sensor

DOI: 10.1002/anie.201001004

A Graphene Oxide–Organic Dye Ionic Complex with DNA-Sensing and Optical-Limiting Properties**

*Janardhan Balapanuru, Jia-Xiang Yang, Si Xiao, Qiaoliang Bao, Maryam Jahan, Lakshminarayana Polavarapu, Ji Wei, Qing-Hua Xu, and Kian Ping Loh**

Graphene oxide (GO), a nonstoichiometric, two-dimensional carbon sheet resulting from acid exfoliation of graphite, offers a new class of solution-dispersible polyaromatic platform for performing chemistry. Graphene oxide bears covalently bound epoxide (1,2-ether) and hydroxyl functional groups on either side of its basal plane, while carboxyl groups are located at the edge sites.[1] Due to the presence of aromatic domains and functional groups, GO undergoes a complex interplay of ionic and nonionic interactions with different molecules in solution.[2–6] Graphene oxide can be considered to be a weak acid cation exchange resin because of the ionizable carboxyl groups, which allow ion exchange with metal cations or positively charged organic molecules. Motivated by the applications of functionalized GO in biosensing[7] and drug delivery,[8] we report a simple ion-exchange strategy for electrostatic complexation of GO with a synthetic dye to form an energy- or charge-transfer complex.[2,4,9] We found that this GO–organic dye charge-transfer complex exhibits enhanced properties for biosensing and optical limiting.

Pyrene derivatives are well known for their noncovalent interactions with molecules having π-electron-rich frameworks.[4,9] To apply them in biosensing, we designed a water-soluble and positively charged dye, namely, 4-(1-pyrenyl-vinyl)-*N*-butylpyridinium bromide (PNPB; for crystal structure, see Supporting Information, Figure S1). This positively charged dye can interact with negatively charged GO to form a fluorescence-quenched charge-transfer complex, named hereafter PNP^+GO^- (Scheme 1). The FTIR spectrum of PNP^+GO^- shows the presence of vibrational features assignable to the functional groups in both GO and PNPB (Supporting Information, S2), and thus attests to successful coupling between them. Atomic force microscopy imaging of PNP^+GO^- shows that a monolayer film can be formed (Supporting Information, S3), which reflects the good monolayer dispersion of PNP^+GO^-. The operating principle of the

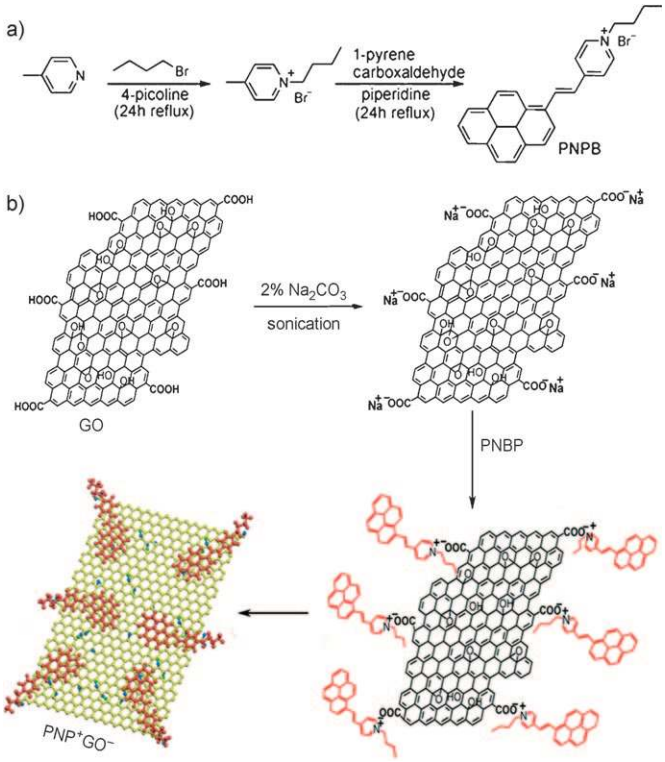

Scheme 1. a) Synthesis of PNPB. b) Ion-exchange process.

PNP^+GO^- sensing platform is based on the unique electrostatic and noncovalent interactions between the analyte and PNP^+, which will "turn on" the quenched fluorescence. The selectivity of PNP^+GO^- for double-stranded DNA over other biomolecules was tested with proteins, RNA, carbohydrates, and surfactants.

As shown in Scheme 1 b, the carboxyl protons at the edges of GO first undergo ion exchange with Na^+, and subsequently with PNP^+. Once PNP^+ is linked to the edges or basal planes of GO, it can also undergo π–π interactions with GO via its pyrene moiety.[4] As a result, the fluorescence of the resultant PNP^+GO^- complex is quenched immediately due to strong charge-transfer interactions between PNP^+ and GO.[2,4,9] Figure 1 a shows the UV/Vis spectra of PNP^+GO^-. The absorption peaks are slightly broadened and red shifted: from free PNPB to bound PNP^+GO^-, the peak shifts from 431 to 446 nm ($\Delta\lambda = 15$ nm), and the absorption peak of GO from 230 to 238 nm ($\Delta\lambda = 8$ nm). This is indicative of strong ionic and π–π interactions between PNP^+ and GO.[4] To reveal the range of concentrations in which PNP^+GO^- exhibits good dispersion in water, we plotted the absorbance at 238 nm

[*] J. Balapanuru, J.-X. Yang, S. Xiao, Q. L. Bao, M. Jahan, L. Polavarapu, Prof. Q. H. Xu, Prof. K. P. Loh
Department of Chemistry, National University of Singapore
3 Science Drive 3, Singapore 117543 (Singapore)
Fax: (+65) 6779-1691
E-mail: chmlohkp@nus.edu.sg
Prof. J. Wei
Department of Physics, National University of Singapore
Singapore 117543 (Singapore)

[**] This work is supported by NRF-CRP grant "Graphene Related Materials and Devices". (R-143-00-360-281).

Supporting information for this article is available on the WWW under http://dx.doi.org/10.1002/anie.201001004.

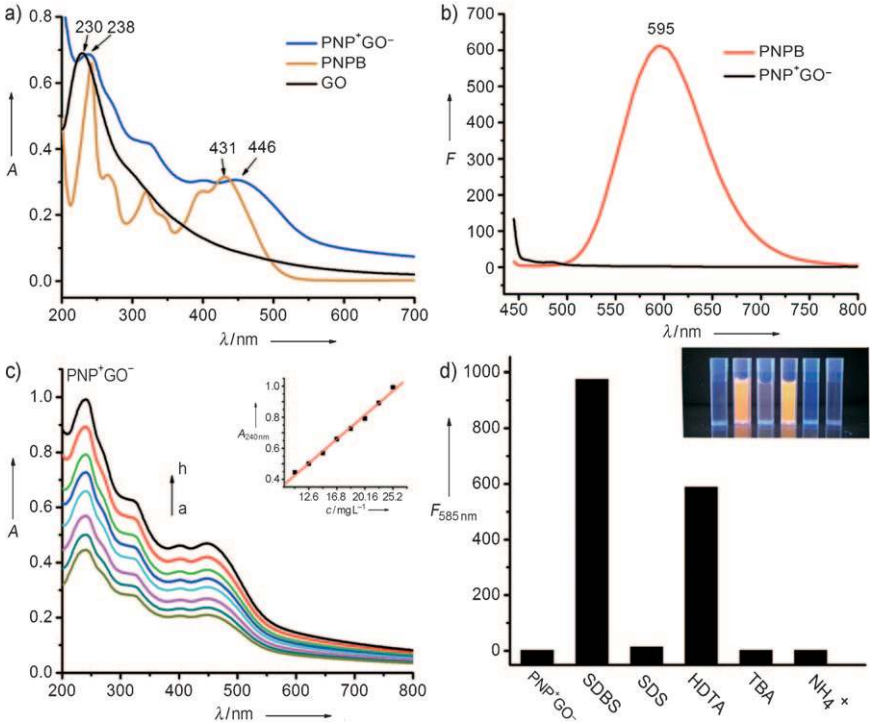

Figure 1. a) UV/Vis absorption spectra of aqueous solutions of PNP^+GO^- (ca. 20 mg L^{-1}), PNPB (2×10^{-6} M), and GO (ca. 34 mg L^{-1}). b) Fluorescence spectra of PNP^+GO^- (ca. 20 mg L^{-1}) and PNPB (2×10^{-6} M). c) Concentration-dependent UV/Vis absorption spectra of PNP^+GO^- from 11.2 to 25.2 mg L^{-1} (a–h, respectively). The inset shows the plot of optical density at 238 nm versus concentration [mg L^{-1}]. d) Comparative fluorescence intensities of PNP^+GO^- (10 mg L^{-1}) complexed with different surfactants at equal concentrations of 1 mM and fluorescence under UV light (inset).

against the concentration of PNP^+GO^- (Figure 1c). Beer's law was used to estimate the effective extinction coefficient of PNP^+GO^- from the slope of the linear least-squares fit, and it was found to be 0.077 L mg^{-1} cm^{-1} with an R value of 0.997. The linear relationship between concentration and absorbance proves homogenous dispersion of PNP^+GO^- in aqueous media. The PNP^+GO^- complex is also soluble in common organic solvents such as *o*-dichlorobenzene, ethanol, THF, and DMF.

The fluorescence spectra of PNP^+GO^- and PNPB (Figure 1b) reveal the exited-state interactions of GO and PNP^+. Almost complete quenching of fluorescence for PNP^+GO^- solution is observed, brought about by photoinduced electron or energy transfer (see Supporting Information, S5), similar to that previously reported for polymer composites of carbon materials such as GO[10] and C_{60}.[11]

Cation exchange of PNP^+GO^- or strong anion–PNP^+ attraction can release PNP^+ from the bound complex, and this turn on the fluorescence from the default off state due to quenching. A systematic study was performed to investigate the roles of positively and negatively charged species in turning on the fluorescence of the PNP^+GO^- complex. These include the negatively charged sodium dodecylbenzenesulfonate (SDBS) and sodium dodecylsulfonate (SDS) as well as the positively charged hexadecyltrimethylammonium bromide (HDTA) and tetrabutylammonium iodide (TBA; see Supporting Information S4 for their structures).

The plot of fluorescence intensity recovery in Figure 1d shows that SDBS is much more efficient in turning on the fluorescence than SDS. From this, we deduce that, besides electrostatic interactions, noncovalent interactions (here due to the π-electron clouds of the

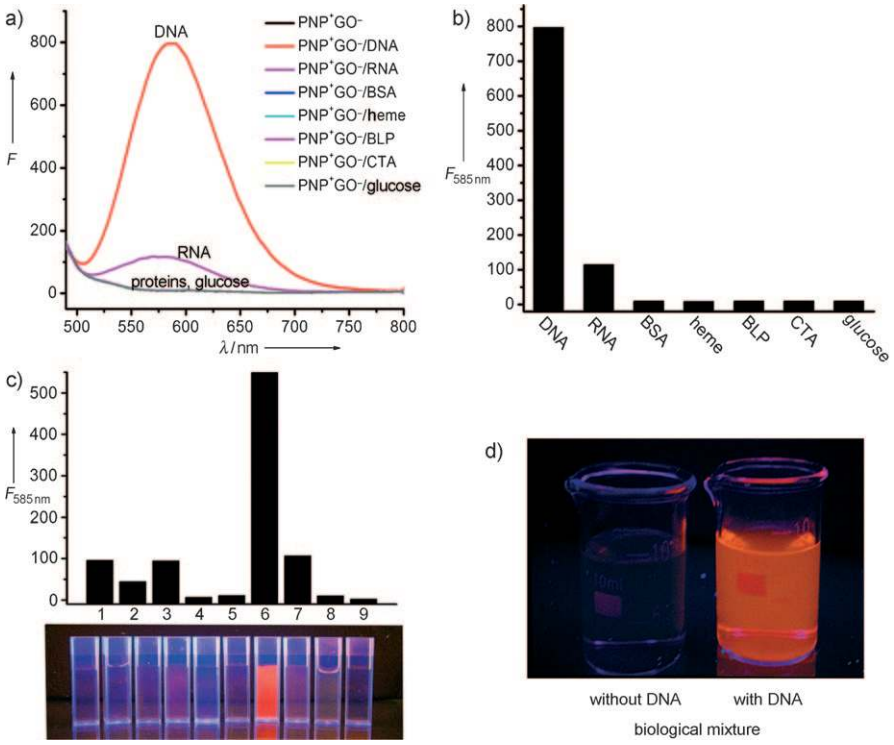

Figure 2. a) Fluorescence spectra and b) comparative intensities of PNP^+GO^- (10 mg L^{-1}) complexed with DNA, RNA, proteins (BSA, heme, BLP, CTA), and glucose at equal concentrations of 20 μM. c) Selectivity studies with different surfactants and biomolecules: 1) SDBS, 2) SDS, 3) HDTA, 4) TBA, 5) NH_4OH, 6) DNA, 7) RNA, 8) BLP, and 9) glucose and their images under UV light. d) Image of PNP^+GO^- complexed with biological mixture of RNA, BSA, glucose, with and without DNA, under UV light.

benzene ring in SDBS) are also crucial to release PNP^+ from the complex.

The interplay of noncovalent and electrostatic interactions in PNP^+GO^- may impart selectivity towards certain biomolecules. Hence, the next step was to investigate whether PNP^+GO^- is selective for DNA, RNA, proteins, and mono/polysaccharides, which are commonly present in blood serum or cell extract. The experiments were carried out with the sodium salt of double-stranded DNA extracted from salmon testes, RNA from baker's yeast, bovine serum albumin (BSA), hemoglobin from bovine blood cells (heme), lens protein from bovine eye (BLP), α-cymo-trypsinogen-A (CTA), and D-(+)-glucose.

Figure 2a shows fluorescence spectra of PNP^+GO^- complexed with different biomolecules at equal concentrations. The fluorescence-enhancing capability of DNA is eight to ten times higher than those of RNA, proteins, and glucose (Figure 2b).

The main reason for the selectivity of PNP^+GO^- for double-stranded DNA is the higher energy of ion-complex formation of PNP^+DNA^- compared to PNP^+GO^-. Being a large and supercharged molecule, DNA has a greater ionic attraction for PNP^+ than the weakly ionizable GO (more weakly charged than DNA), and thus ion exchange can proceed as illustrated in Scheme 2.

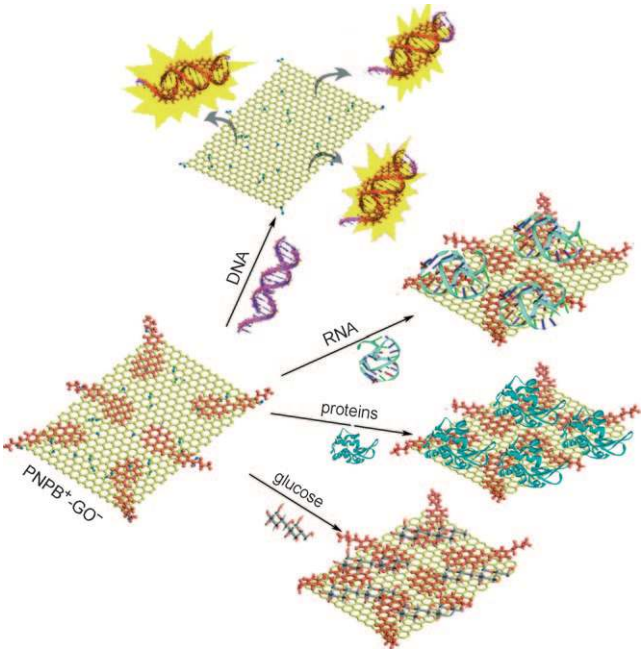

Scheme 2. Sensing by PNP^+GO^-. DNA can complex efficiently with PNP^+ to form ionic complex PNP^+DNA^-, and thus switches on the fluorescence. Other biomolecules undergo π–π stacking on GO but do not remove PNP^+ from GO, and thus fluorescence remains quenched.

A control study carried out by adding GO to preformed ion complex PNP^+DNA^- shows that GO has a minimal quenching effect on PNP^+DNA^- (Supporting Information, S4). This provides direct evidence that the electrostatic bonding between PNP^+ and DNA^- is stronger than that of PNP^+ and GO^-. An important finding is that the PNP^+GO^- complex is selective for DNA over other biomolecules. Even though RNA is made up of similar nucleotides to DNA (except for thymine), it is not as efficient as DNA in turning on the quenched fluorescence. The single-stranded and supercoiled structure of RNA allows it to undergo π–π stacking on the GO surface, but its complex-formation energy with PNP^+ is not sufficiently high to remove it from GO.[7]

The PNP^+GO^- complex can be used to detect traces of DNA present in a given biological mixture (Figure 2d). A linear relation was observed between the fluorescence

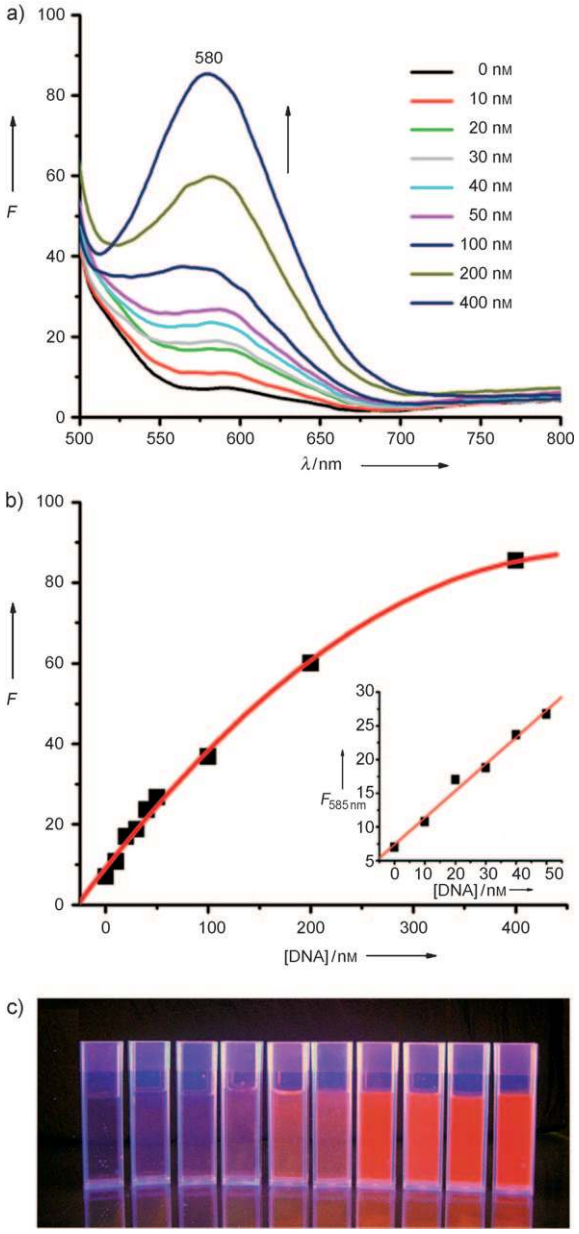

Figure 3. a) Fluorescence spectra of PNP^+GO^- complexed with different concentrations of DNA ranging from 10 to 400 nM b) Calibration plot of fluorescence intensity at 580 nm versus concentration of DNA [nM]. The inset shows the calibration plot at low concentrations of DNA (up to 50 nM). c) Image of PNP^+GO^- complexed with different concentrations of DNA under UV light.

intensity and the amount of DNA (Figure 3). Such quantitative detection is very useful for determining the amplification yield of the polymerase chain reaction (PCR) before sequencing[12] and to identify contaminant DNA in recombinant protein products.[13] Most importantly, unlike other, toxic assays for DNA quantification such as ethidium bromide or PicoGreen, this cost-effective graphene-based powder is thermally quite stable and safe to handle. Moreover, the specific interactions between DNA and PNP^+GO^- made rapid and selective detection of DNA with a detection limit of 1 nM possible in this experiment.

Nonlinear optical effects can arise from charge-transfer complexes because of the possibility of multiphoton absorption in the dye, which can give rise to reverse saturable absorption effects in optical limiting.[14] Alternatively, rapid absorption of laser energy by the dye and efficient energy transfer to GO can lead to the ionization of GO sheets, which forms rapidly expanding microplasmas. These microplasmas strongly scatter light from the transmitted beam direction, and this leads to a decrease in the measured transmitted light energy.[15]

The nonlinear transmittance of solutions of GO, PNPB, and PNP^+GO^- in deionized water was studied with nanosecond laser pulses (7 ns) at 532 and 1064 nm. The linear transmittances of PNP^+GO^- are 63 and 74% at 532 and 1064 nm, respectively. Figure 4a shows that, at lower input fluences, there is no significant change in the transmittance of GO, PNPB, and PNP^+GO^-, but when the input fluence is increased beyond a certain threshold energy, the transmittance of PNP^+GO^- decreases, that is, it shows an optical-limiting property. The nonlinear transmission of PNP^+GO^- starts at 0.21 $J\,cm^{-2}$, which is much lower than those of individual GO (1.51 $J\,cm^{-2}$) and PNPB (1.50 $J\,cm^{-2}$) but comparable to that of graphene–oligothiophene composite (0.15 $J\,cm^{-2}$).[16] At 532 nm, the limiting threshold value (the input fluence at which the transmittance falls to 50% of the linear transmittance) of PNP^+GO^- is 1.55 $J\,cm^{-2}$; this is much improved from pure GO and better than that of the benchmark optical liming material C_{60} (3.0 $J\,cm^{-2}$) measured on the same system.[17] Compared to reported graphene composites, in which the optical limiting is mainly effective in the visible region,[10,16,18] one advantage is that the optical-limiting behavior of PNP^+GO^- can be extended to the near-infrared range. Figure 4b shows the optical-limiting responses of the PNP^+GO^-, GO, and PNPB solutions at 1064 nm. When the incident laser fluence exceeds 2 $J\,cm^{-2}$, an abrupt drop in transmittance is observed for PNP^+GO^- solution at a limiting threshold of 8.10 $J\,cm^{-2}$. At 1064 nm the optical-limiting performance of PNP^+GO^- is better than that of carbon nanotubes (10 $J\,cm^{-2}$) measured on the same system.[19] Thus such graphene oxide–organic dye ionic complexes have potential as broadband optical limiters.

Figure 4c and d show the dependence of the scattering signals, collected at an angle of 40° to the propagation axis of the transmitted laser beam at 532 and 1064 nm, on input laser fluence. As the input fluence increases, the scattering signals of PNP^+GO^- deviate from linear behavior.

Figure 4e and f show the scattered signals at different angles (every 5° from 10 to 160°) with respect to the transmitted laser beam for PNP^+GO^-, GO, and PNPB at an

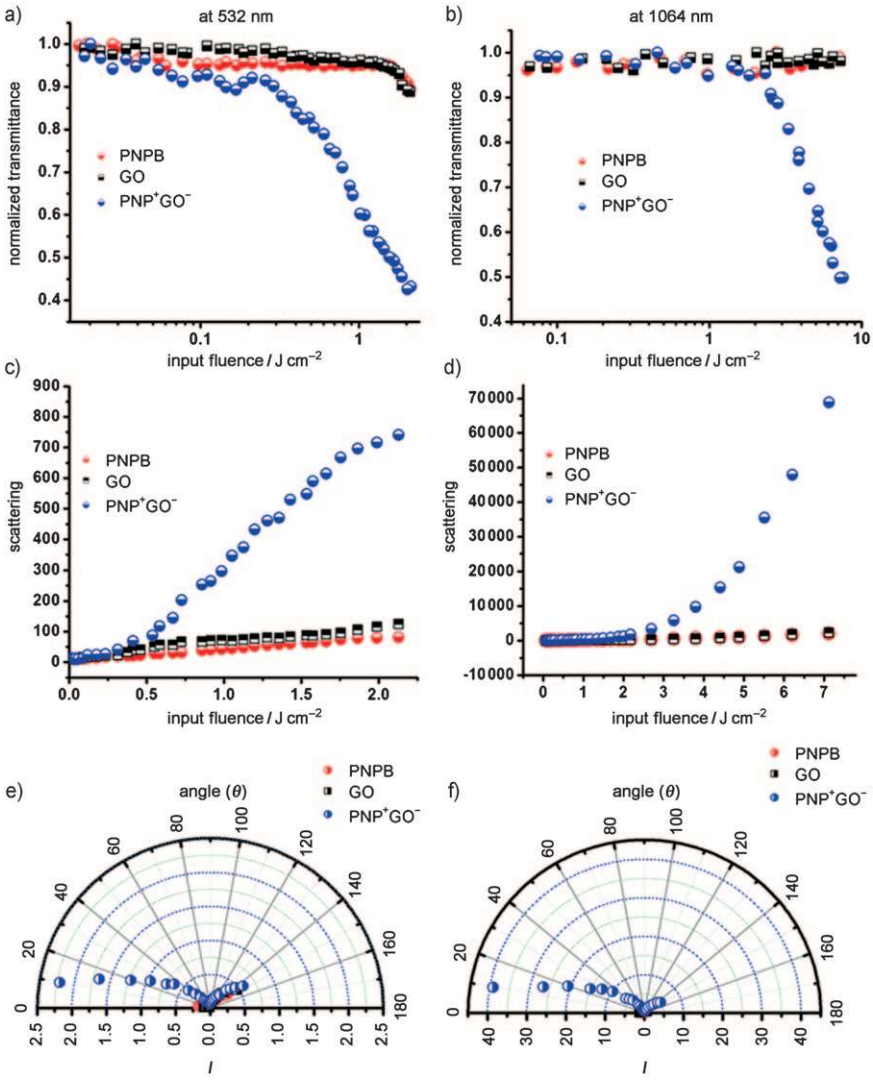

Figure 4. Optical limiting response of aqueous solutions of PNP^+GO^- (20 $mg\,L^{-1}$), GO (34 $mg\,L^{-1}$), and PNPB (2×10^{-6} M), measured with 7 ns laser pulses at a) 532 and b) 1064 nm. Nonlinear scattering response of PNP^+GO^-, GO and PNPB solutions at laser pulses of 532 (c and e) and 1064 nm (d and f), where c) and d) show intensity-dependent scattering signals at 532 and 1064 nm, respectively, and e) and f) angle-dependent scattering signals at 532 and 1064 nm respectively.

incident intensity of 1.4 J cm^{-2} for 532 nm laser pulses and 5.0 J cm^{-2} for 1064 nm laser pulses. The scattered light signals for PNP^{+}GO^{-} are significantly larger than those of GO and PNPB in both forward and backward scattering. The scattering signals for PNP^{+}GO^{-} occur below 20° for 532 and 1064 nm.

Since increased scattering intensity results in decreased transmission, nonlinear scattering appears to be responsible for the optical limiting here. Similar to the optical-limiting mechanisms of carbon black[20] and carbon nanotubes,[21] the limiting behavior of PNP^{+}GO^{-} is mainly caused by two types of scattering centers that exist after photoexcitation of PNP^{+}GO^{-}. When the laser is focused on PNP^{+}GO^{-}, rapid transfer of the excitation energy absorbed by the dye (PNPB) molecules to the GO sheets results in PNP^{+}GO^{-} microplasmas which act as primary scattering centers, and the microplasma is dissipated to the surrounding solvent. Consequently, the solvent is heated and forms microbubbles, which act as secondary scattering centers for input laser pulses.[15]

In conclusion, we have synthesized a graphene oxide–dye charge-transfer complex by a simple ion-exchange process. We demonstrate that the GO–dye complex can be used as an optical sensor for DNA, for which it is selective over a variety of commonly used surfactants and biomolecules. Unlike other toxic assays used for DNA quantification, no special precautions were required to handle this thermally stable graphene-based powder. The GO–dye complex also shows good broadband optical-limiting properties. Hence, this work inspires the development of multifunctional GO-based hybrid materials through a simple ion-exchange process involving the ionizable functional groups in GO. The concept can be extended to the creation of strong or weak acid groups on GO by functionalizing it with other acidic groups, for example, sulfonate groups. Taking advantage of the high surface area of GO, potential applications of such GO ionic complexes also include ion-exchange resins for treating wastewater and sustained drug release, in addition to what has been demonstrated here.[22]

Received: February 17, 2010
Revised: June 24, 2010
Published online: July 27, 2010

Keywords: charge-transfer complexes · graphene oxide · ion exchange · nonlinear optics · sensors

[1] a) D. A. Dikin, S. Stankovich, E. J. Zimney, R. D. Piner, G. H. B. Dommett, G. Evmenenko, S. T. Nguyen, R. S. Ruoff, *Nature* **2007**, *448*, 457–460; b) K. P. Loh, Q. L. Bao, P. K. Ang, J. X. Yang, *J. Mater. Chem.* **2010**, *20*, 2277–2289.
[2] Y. Y. Liang, D. Q. Wu, X. L. Feng, K. Müllen, *Adv. Mater.* **2009**, *21*, 1679–1683.
[3] S. Niyogi, E. Bekyarova, M. E. Itkis, J. L. McWilliams, M. A. Hamon, R. C. Haddon, *J. Am. Chem. Soc.* **2006**, *128*, 7720–7721.
[4] Y. X. Xu, H. Bai, G. W. Lu, C. Li, G. Q. Shi, *J. Am. Chem. Soc.* **2008**, *130*, 5856–5857.
[5] X. L. Li, G. Y. Zhang, X. D. Bai, X. M. Sun, X. R. Wang, E. G. Wang, H. J. Dai, *Nat. Nanotechnol.* **2008**, *3*, 538–542.
[6] Y. C. Si, E. T. Samulski, *Nano Lett.* **2008**, *8*, 1679–1682.
[7] a) C. H. Lu, H. H. Yang, C. L. Zhu, X. Chen, G. N. Chen, *Angew. Chem.* **2009**, *121*, 4879–4881; *Angew. Chem. Int. Ed.* **2009**, *48*, 4785–4787; b) S. J. He, B. Song, D. Li, C. F. Zhu, W. P. Qi, Y. Q. Wen, L. H. Wang, S. P. Song, H. P. Fang, C. H Fan, *Adv. Funct. Mater.* **2010**, *20*, 453–459; c) N. Mohanty, V. Berry, *Nano Lett.* **2008**, *8*, 4469–4476.
[8] Z. Liu, J. Robinson, X. M. Sun, H. J. Dai, *J. Am. Chem. Soc.* **2008**, *130*, 10876–10877.
[9] R. S. Swathi, K. L. Sebastian, *J. Chem. Phys.* **2008**, *129*, 054703.
[10] Y. S. Liu, J. Y. Zhou, X. L. Zhang, Z. B. Liu, X. J. Wan, J. G. Tian, T. Wang, Y. S. Chen, *Carbon* **2009**, *47*, 3113–3121.
[11] P. A. Van hal, J. Knol, B. M. W. Langeveld-Voss, S. C. J. Meskers, J. C. Hummelen, R. A. J. Janssen, *J. Phys. Chem. A* **2000**, *104*, 5974–5988.
[12] R. B. Chadwick, M. P. Conrad, M. D. McGinnis, L. Johnston-Dow, S. L. Spurgeon, M. N. Kronick, *Biotechniques* **1996**, *20*, 676–683.
[13] R. Bolger, F. Lenoch, E. Allen, B. Meiklejohn, T. Burke, *Biotechniques* **1997**, *23*, 532–537.
[14] R. L. Sutherland, *Handbook of Nonlinear Optics*, 2nd ed., Marcel Dekker, New York, **2003**.
[15] J. Wang, Y. Hernandez, M. Lotya, J. N. Coleman, W. J. Blau, *Adv. Mater.* **2009**, *21*, 2353–2448.
[16] X. L. Zhang, X. Zhao, Z. B. Liu. Y. S. Chen. J. G. Tian, *Opt. Express* **2009**, *17*, 23959–23964.
[17] H. I. Elim, J. Y. Ouyang, S. H. Goh, W. Ji, *Thin Solid Films* **2005**, 477, 63–72.
[18] Y. F. Xu, Z. B. Liu, X. L. Zhang, Y. Wang, J. G. Tian, Y. Huang, Y. F. Ma, X Y. Zhang, Y. S. Chen, *Adv. Mater.* **2009**, *21*, 1275–1279.
[19] L. Polavarapu, N. Venkatram, W. Ji. Q. H. Xu, *ACS Appl. Mater. Interfaces* **2009**, *1*, 2298–2303.
[20] K. Mansour, M. J. Soileau, E. W. Van Stryland, *J. Opt. Soc. Am. B* **1992**, *9*, 1100–1109.
[21] J. Wang, W. J. Blau, *J. Phys. Chem. C* **2008**, *112*, 2298–2303.
[22] S. D. Alexandratos, *Ind. Eng. Chem. Res.* **2009**, *48*, 388–398.

